JACS
JOURNAL OF THE AMERICAN CHEMICAL SOCIETY
Article
pubs.acs.org/JACS

The Role of Arene−Arene Interactions in the Folding of *ortho*-Phenylenes

Sanyo M. Mathew,[†] James T. Engle,[‡] Christopher J. Ziegler,[‡] and C. Scott Hartley*[,†]

[†]Department of Chemistry & Biochemistry, Miami University, Oxford, Ohio 45056, United States
[‡]Department of Chemistry, University of Akron, Akron, Ohio 44325, United States

Supporting Information

ABSTRACT: The *ortho*-phenylenes are a simple class of helical oligomers and representative of the broader class of sterically congested polyphenylenes. Recent work has shown that *o*-phenylenes fold into well-defined helical conformations (in solution and, typically, in the solid state); however, the specific causes of this folding behavior have not been determined. Here, we report the effect of substituents on the conformational distributions of a series of *o*-phenylene hexamers. These experiments are complemented by dispersion-corrected DFT calculations on model oligomers (B97-D/TZV(2d,2p)). The results are consistent with a deterministic role for offset arene−arene stacking interactions on the folding behavior. On the basis of the experimental and computational results, we propose a model for *o*-phenylene folding with two simple rules. (1) Conformers are forbidden if they include a particular sequence of biaryl torsional states that causes excessive steric strain. These "ABA" states correspond to consecutive dihedral angles of −55°/+130°/−55° (or +55°/−130°/+55). (2) The stability of the remaining conformers is determined by offset arene−arene stacking interactions that are easily estimated as an additive function of the number of well-folded torsional states (±55°) along the backbone. For the parent, unsubstituted poly(*o*-phenylene), each interaction contributes roughly 0.5 kcal/mol to the helix stability (in chloroform), although their strength is sensitive to substituent effects. The behavior of the *o*-phenylenes as a class is discussed in the context of this model. They are analogous to α-helices, with axial aromatic stacking interactions in place of hydrogen bonding. The model predicts that the overall folding propensity should be quite sensitive to relatively small changes in the strength of the arene−arene stacking. In a broader sense, these results demonstrate that polyphenylenes may exhibit folding behavior that is amenable to simple models, and validate the use of diffusion-corrected DFT methods in predicting their three-dimensional structures.

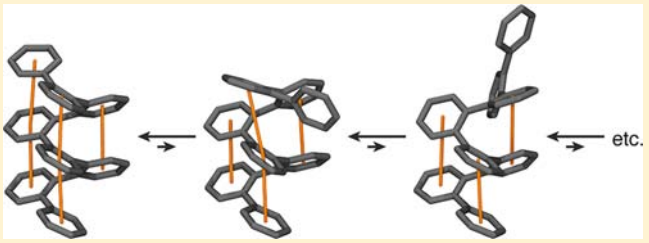

INTRODUCTION

The polyphenylenes,[1−3] architectures based on directly connected aromatic rings, are inherently conjugated and chemically robust;[4] consequently, they are an important class of compounds for applications in materials science and nanotechnology. The best-known examples of polyphenylenes are *para*-phenylene polymers and oligomers,[5] which have been used in organic electronics[6] (particularly as emissive materials)[7] and as single molecule wires.[8] While *p*-phenylenes are essentially rigid rods (and can be very useful as structural units[9]), the incorporation of *ortho* and *meta* linkages, possibly in combination with branching, gives polyphenylenes with more complex three-dimensional structures. Thus, *m*-phenylenes have been used as helical polymers[10,11] and oligomers[12] with applications in molecular recognition.[13,14] Similarly, highly branched polyphenylene dendrimers[15] have been used as platforms for controlled energy transfer.[16,17]

The *o*-phenylenes, one of the most fundamental types of polyphenylene, have recently received increasing attention. Building on the few reports of *o*-phenylenes prior to 2010,[18−20] our own work has shown that *o*-phenylenes exhibit weak delocalization that is quite sensitive to substituent effects.[21−23] We have also shown that short *o*-phenylene oligomers are strongly predisposed to folding into well-defined helical conformations in solution, although, in general, they exhibit conformational disorder at their ends.[24] Likewise, Fukushima and Aida have reported a remarkable helical *o*-phenylene oligomer that spontaneously resolves in the solid state and undergoes a large decrease of its racemization rate on oxidation.[25] More recently, they have demonstrated a surprising solvent effect whereby acetonitrile appears to uniquely promote the folding of their oligomers into "perfect" helices (i.e., without end-group disorder).[26] This phenomenon has been attributed to a steric effect in a general sense, but to our knowledge, its precise origin is currently undetermined.

Thus, while not necessarily useful as conjugated polymers in the conventional sense, the *o*-phenylenes represent a new class of helical polymers[27,28] and foldamers.[29−31] Interest in other, related sterically congested polyphenylene architectures also appears to be increasing; for example, Dichtel[32] and Manabe[33] have recently reported examples of alternating *o*/*p* and *o*/*o*/*p*

Received: March 13, 2013
Published: April 4, 2013

   dx.doi.org/10.1021/ja4026006 | J. Am. Chem. Soc. 2013, 135, 6714−6722

polyphenylenes, respectively. In both cases, twisting from the *ortho* linkages is implicated in the adoption of compact conformations and there is at least the potential for interesting secondary structures. However, experimental determination of the precise folding behavior of these compounds is challenging, and it remains to be determined whether these sorts of motifs adopt (or can be made to adopt) well-defined three-dimensional structures.

Ultimately, linear (unbranched) polyphenylenes with various sequences of *ortho*, *meta*, and *para* linkages may, by analogy with biomolecules, be made to fold into complex tertiary structures. Further, understanding the conformational preferences of polyphenylenes may be important to understanding the complex factors influencing their use[34−36] as precursors to nanographenes via the Scholl reaction. However, our understanding of the interactions involved in polyphenylene folding is in its infancy: *o*-phenylene helices have been demonstrated but not explained, and the behavior of other types of repetitive linear oligo(phenylene) sequences is much less clear. The conformational analysis of these simple oligomers is deceptively complex, involving, in principle, both the inherent torsional preferences of each biaryl bond and a number of different possible face-to-face and edge-to-face arene−arene interactions. Unfortunately, computational modeling of polyphenylene segments is made more difficult by the failure of commonly used computational methods to correctly predict their relative conformational stabilities.[22]

Here, we report a systematic investigation of substituent effects on the conformational behavior of *o*-phenylenes. Hexamers **oP^6(X)$_2$** were chosen as targets because they are sufficiently long that conformational exchange is slow on the NMR time scale,[22] but also sufficiently short that their NMR spectra can be completely analyzed to provide quantitative and complete conformational distributions. The substituents (NMe_2, Me, H, F, CF_3, CN, NO_2) were varied at the oligomer ends both for synthetic convenience and because these positions were expected to be more sensitive to substituent effects.[23] The oligomers do indeed exhibit distinct conformational distributions, which can be rationalized in the context of model systems for the study of arene−arene interactions. The experimental results also validate the use of the diffusion-corrected B97-D DFT method for the prediction of relative conformer stabilities. By combining the experimental and computational results, we propose a very simple, semiquantitative model for the folding of *o*-phenylenes that clarifies the role of arene−arene interactions in determining their behavior and rationalizes several of their reported properties. The model provides guidelines for the design of new *o*-phenylenes with high folding propensities. These results should also be applicable to the analysis of congested polyphenylenes more generally.

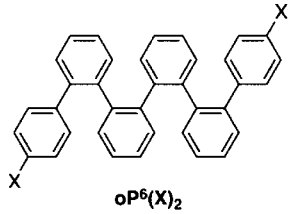

oP^6(X)$_2$
X = H, Me, NMe_2, NO_2, CN, CF_3, F

RESULTS AND DISCUSSION

Synthesis. Our synthesis of the **oP^6(X)$_2$** series is a straightforward modification of our previously developed approach to *o*-phenylenes[21,22] and is shown in Scheme 1. Briefly, Suzuki−Miyaura coupling of known boroxarene **1**[37] and 2-(2-bromophenyl)phenol

Scheme 1. Synthesis of oP^6(X)$_2$[a]

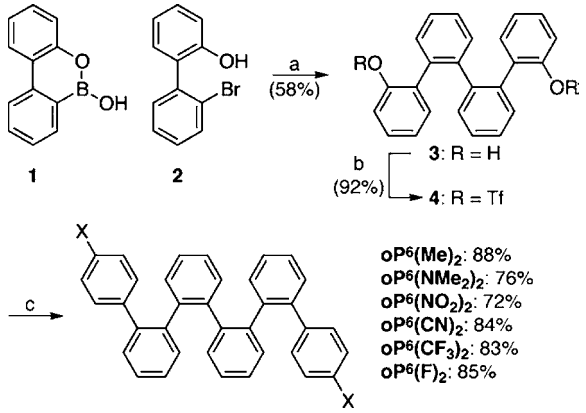

[a]Reagents and conditions: (a) $Pd(PPh_3)_4$, Na_2CO_3(aq), THF/H_2O (4:1), Δ; (b) Tf_2O, pyridine, CH_2Cl_2; (c) arylboronic acid, $Pd(OAc)_2$, SPhos, K_3PO_4, THF/H_2O (4:1), Δ.

2[38] gave symmetrical *o*-phenylene tetramer diol **3**, which was converted to ditriflate **4** in good yield. The target series of hexamers was then prepared by Suzuki−Miyaura coupling with the appropriate phenylboronic acid derivatives in good yields. Full details are given in the Supporting Information. As is common for *o*-phenylenes, the NMR spectra of the final compounds are complex because of slow conformational exchange; however, they were fully assigned to the proposed structures as described below. X-ray quality single-crystals were grown of four of the compounds, **oP^6(NMe$_2$)$_2$** (DCM/hexanes), **oP^6(Me)$_2$** ($CDCl_3$/hexanes), **oP^6(NO$_2$)$_2$** (EtOH/DCM), and **oP^6(CF$_3$)$_2$** (DCM/EtOH). The resulting crystal structures are shown in Figure 1. All four oligomers crystallize into very similar

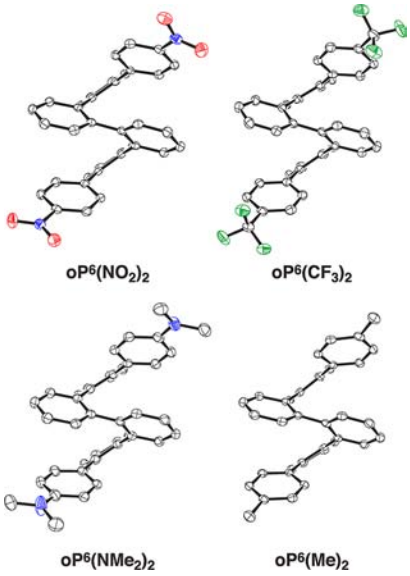

Figure 1. ORTEP representations (50% ellipsoid probability) of the crystal structures of **oP^6(NO$_2$)$_2$**, **oP^6(CF$_3$)$_2$**, **oP^6(NMe$_2$)$_2$**, and **oP^6(Me$_2$)$_2$**. Hydrogen atoms have been omitted for clarity.

quasi-C_2-symmetric helical conformers, as has been observed for some (but not all) other *o*-phenylene hexamers.[25,26,39] The unit

dx.doi.org/10.1021/ja4026006 | J. Am. Chem. Soc. 2013, 135, 6714−6722

cells of all of the compounds comprise both enantiomeric helices in all cases.

Conformational Analysis. For simple *o*-phenylene hexamers, such as $\mathbf{oP^6(X)_2}$, the backbone conformation is dictated by the internal dihedral angles ϕ_2, ϕ_3, and ϕ_4, shown in Figure 2.

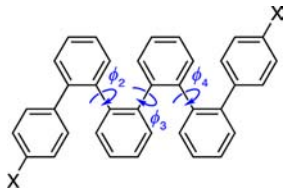

Figure 2. Key dihedral angles in the folding of $\mathbf{oP^6(X)_2}$.

Within a single *o*-phenylene strand, each of these can assume one of two possible values: $\phi_i \approx -55°$ or $\phi_i \approx +130°$. We refer to these as the "A" and "B" states, respectively. Thus, the AAA conformer, with $\phi_2 \approx \phi_3 \approx \phi_4 \approx -55°$,[40] is a compact, left-handed helix with every third ring stacked. All of the solid-state structures shown in Figure 1 correspond to the AAA conformer. There are six, and only six, possible backbone configurations for an *o*-phenylene hexamer: four that are C_2-symmetric (AAA, BAB, BBB, ABA) and two that are unsymmetric (AAB and ABB), as shown in Figure 3 for

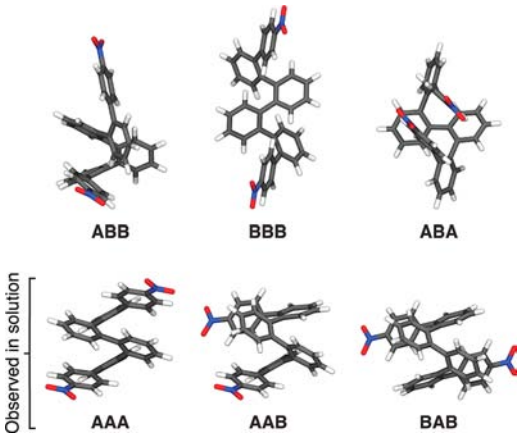

Figure 3. Backbone conformers available to $\mathbf{oP^6(NO_2)_2}$. The geometries were optimized at the B97-D/TZV(2d,2p) level.

$\mathbf{oP^6(NO_2)_2}$. Of course, there is a degenerate, enantiomeric counterpart for each of these states with A′ = +55° and B′ = −130°. In this study, none of the compounds have been resolved and thus all observed conformers are racemates. Note, however, that the two enantiomeric pools are distinct:[24] a single molecule can have A/B states or A′/B′ states but no A/A′ and B/B′ mixtures. Conformational exchange between different backbone conformers (e.g., AAA ⇄ AAB ⇄ etc.), considered in this study, is faster than, and can be considered independently of, racemization (AAA/AAB/etc. ⇄ A′A′A′/A′A′B′/etc.). A more thorough discussion of these issues was given in an earlier paper.[24]

We have previously shown that, for *o*-phenylene oligomers longer than the pentamer, the backbone conformational states are in slow exchange on the NMR time scale at room temperature and below. Thus, deconvolution and integration of ^{1}H NMR spectra can be used to determine conformational distributions. Simple *o*-phenylenes, such as the parent series,[22] show a preference for the A states: the most populated conformer at room temperature is the compact 3_1 AAA helix. Some disorder occurs at the ends of the oligomers; thus, we believe that the behavior of *o*-phenylenes can be characterized, in general, as well-defined helical cores with disorder occurring primarily at the ends. These conclusions are also consistent with solid-state structures reported by us[21] (see above) and the results of Fukushima and Aida.[25,26]

Unfortunately, the specific interactions responsible for the relative stabilities of the conformers in Figure 3 (or the many analogous conformers for longer *o*-phenylenes) are not obvious. Offset stacking interactions between every third arylene presumably stabilize the "folded" AAA conformer, but the dependence of such stacking interactions and various other (e.g., edge-to-face) interactions on the backbone geometry is not clear. The challenge of analyzing the folding properties of *o*-phenylenes as a class is exacerbated by the exponential increase in the number of possible conformers with increasing length. Further, although DFT geometry optimizations of the oligomers are straightforward, standard DFT methods (e.g., B3LYP) do not correctly predict the relative stabilities of the conformations, incorrectly favoring the B states. This failure is not surprising, as these methods are not expected to predict the strength of arene−arene interactions (and other dispersion-based interactions),[41−43] which, regardless of the particular conformer under consideration, are likely to be very important.

The conformational behavior of the $\mathbf{oP^6(X)_2}$ series in $CDCl_3$ was probed by NMR spectroscopy at 277 K using our previously reported strategy.[24] As expected, the 1D ^{1}H NMR spectra of all of the hexamers are complex, comprising contributions from three slowly exchanging conformational states we label **I**, **II**, and **III** in order of decreasing signal intensity. The ^{1}H NMR spectrum of $\mathbf{oP^6(NO_2)_2}$ is shown in Figure 4, with the others

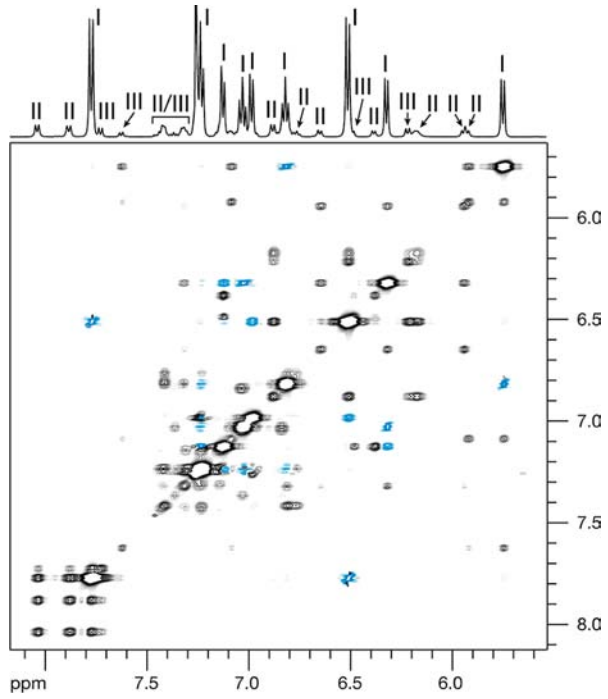

Figure 4. 1D ^{1}H NMR (top) and EXSY spectra of $\mathbf{oP^6(NO_2)_2}$ ($CDCl_3$, 277 K).

provided in the Supporting Information. For each of the compounds, COSY, HMQC, HMBC, and EXSY spectra were

dx.doi.org/10.1021/ja4026006 | J. Am. Chem. Soc. 2013, 135, 6714−6722

obtained. The EXSY spectra, also shown in Figure 4 for $\mathbf{oP^6(NO_2)_2}$, confirm, in all cases, that the purity of the compounds is quite high: the minor signals show cross-peaks with corresponding signals from conformer **I**, indicating that they represent conformers in slow exchange, not impurities. Chemical shift assignments (^{1}H and ^{13}C) for conformer **I** were made using the COSY, HMQC, and HMBC spectra. Chemical shift assignments for the minor conformers, **II** and **III**, were then obtained using the EXSY (and COSY) spectra to map the assignments from **I**. Chemical shift assignments for the complete $\mathbf{oP^6(X)_2}$ series in all three observed conformational states are given in the Supporting Information. On the basis of the number of signals observed in the spectra, it is readily determined that conformers **I** and **III** represent 2-fold-symmetric geometries, whereas conformer **II** is unsymmetrical.

To assign specific geometries to **I**, **II**, and **III**, we compared the experimental chemical shift assignments to those predicted for all six backbone configurations possible for *o*-phenylene hexamers (i.e., Figure 2). For the geometry optimizations, we used the B97-D/TZV(2d,2p) method,[44] a dispersion-corrected DFT method that is now commonly used to quantitatively investigate arene−arene interactions, including substituent effects.[45−47] Gratifyingly, unlike the other DFT methods we have previously employed, the B97-D method correctly predicts the order of stability of the previously observed conformers of $\mathbf{oP^6(H)_2}$ (AAA > AAB > BAB). Relative stabilities of the conformers for each of the $\mathbf{oP^6(X)_2}$ series are given in Figure S1. ^{1}H chemical shifts were calculated for each geometry at the PCM/WP04/6-31G(d) level.[48,49] All three conformers for all members of the $\mathbf{oP^6(X)_2}$ series could be unambiguously matched to one of the optimized geometries: in all cases, the match had the lowest RMS error when compared to the experimental chemical shift data, and the RMS errors were always uniquely below our previously determined standard of 0.15 ppm for *o*-phenylenes using this method. Consistent with our previous results, in all cases conformers **I** correspond to the AAA geometries, conformers **II** correspond to the AAB geometries, and conformers **III** correspond to the BAB geometries. Relative conformer populations were then obtained from the integration of the ^{1}H NMR spectra through deconvolution of relatively uncluttered regions, and are compiled in Table 1.

Table 1. Equilibrium Conformer Populations and ΔG°_{fold} Values for Hexamers $oP^6(X)_2$ in $CDCl_3$ at 277 K

X	AAA	AAB	BAB	ΔG°_{fold} (kcal/mol)[a]
NO_2	74.3	20.6	5.2	−0.71 ± 0.04
CN	74.4	18.2	7.4	−0.77 ± 0.04
CF_3	74.6	21.0	4.4	−0.70 ± 0.04
F	56.6	33.9	9.5	−0.28 ± 0.04
H	49.0	41.7	9.3	−0.09 ± 0.04
Me	41.0	49.0	8.9	+0.10 ± 0.04
$N(Me)_2$	44.1	47.4	8.4	+0.04 ± 0.04

[a]Errors calculated assuming a 5% error on integration of the ^{1}H NMR spectra.

The populations of each conformer are highly substituent-dependent, with, in general, an increasing preference for the AAA conformer when the oligomers are functionalized with electron-withdrawing substituents (NO_2, CN, CF_3). We chose to focus on the folding reaction AAB ⇄ AAA with a free energy change ΔG°_{fold}, as the populations of these two conformers were typically large enough to allow quantitative integration. In the absence of stabilizing effects such as arene−arene stacking, ΔG°_{fold} would be +0.38 kcal/mol ($-RT\ln(1/2)$) because of the reduced symmetry of the AAB conformer (i.e., both ends of the oligomer are equivalent; therefore, statistically, a 2:1 AAB:AAA ratio would be expected). Thus, in *all* cases, the AAA conformer is stabilized by 0.3−1.1 kcal/mol (at 277 K) relative to a hypothetical unbiased freely mobile oligomer.

The ΔG°_{fold} values show a good linear dependence on the Hammett constants σ_m for the terminal substituents,[50] as shown in Figure 5, with $r = -0.96$, representing a strong, statistically

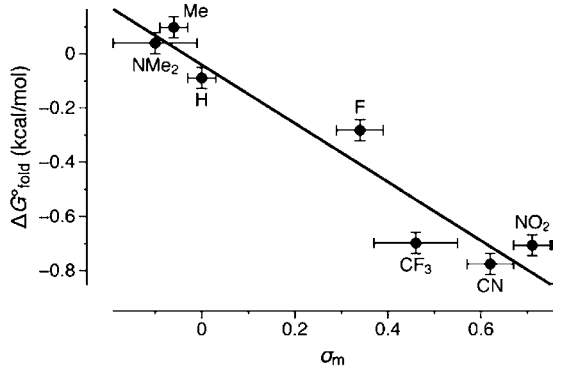

Figure 5. ΔG°_{fold} plotted against σ_m for $\mathbf{oP^6(X)_2}$ ($CDCl_3$, 277 K).

significant correlation ($p = 0.0005$). As discussed in more detail below, the behavior of these short oligomers is reminiscent of molecular torsion balances used to study quasi-intermolecular interactions (including arene−arene interactions).[51,52] The quality of the correlation between ΔG°_{fold} and σ_m is typical of similar systems which were designed explicitly to quantify arene−arene interactions, including face-to-face stacking measured in 1,8-diarylnaphthalenes[53] or chemical double mutant cycles[54,55] and related systems examining edge-to-face interactions.[56]

The experimental ΔG°_{fold} data was then compared to the B97-D/TZV(2d,2p) energy differences ΔE_{fold} between the AAB and AAA geometries, as shown in Figure 6. Of course, our goal here is

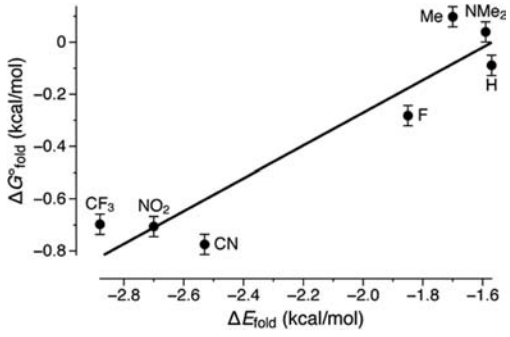

Figure 6. Experimental ΔG°_{fold} plotted against computational ΔE_{fold}.

not quantitative prediction of the experimental results. Considering the relatively small substituent effect ($\Delta\Delta G^\circ_{fold} <$ 0.9 kcal/mol), and that solvation and ΔS° are not at all treated by these (gas-phase) calculations, the calculated stabilities do a good job of accounting for the substituent effects in the series, with a correlation coefficient of $r = 0.94$ ($p = 0.0016$). The roughly 1.5−2 kcal/mol difference between ΔE_{fold} and ΔG°_{fold} is

dx.doi.org/10.1021/ja4026006 | J. Am. Chem. Soc. 2013, 135, 6714−6722

consistent with previous efforts to compare B97-D calculations to experimental models of aromatic stacking in chloroform.[47,57] The difference likely comprises 0.4 kcal/mol for the entropic bias toward AAB (see above) and 1−1.5 kcal/mol for changes in solvation (and other factors). Since the AAB geometry should expose more molecular surface to the solvent, a change in solvation energy of 1−1.5 kcal/mol would appear to be reasonable given that the free energy of solvation of benzene in chloroform is −4.6 kcal/mol.[58] Unfortunately, the limited solubility of the $\mathbf{oP^6(X)_2}$ compounds in polar solvents precluded the investigation of their conformational behavior in other media. However, we did examine the behavior of $\mathbf{oP^6(H)_2}$ in toluene-d_8; the conformational distribution is the same to that in $CDCl_3$ within experimental error (53:40:8 AAA:AAB:BAB). The most striking difference between the calculated energies and the observed experimental free energies of folding is that the calculations predict that all substituents should have a stabilizing effect relative to the unsubstituted case $\mathbf{oP^6(H)_2}$, whereas the electron donating substituents (Me, NMe_2) were observed experimentally to decrease the population of the helical conformer. This discrepancy is, however, too small for us to say whether it derives from a genuine failure by the calculations or an unaccounted-for substituent effect (on solvation, for example).

Arene−Arene Interactions and *o*-Phenylene Folding. On the basis of these results, we propose that the determining factor controlling conformational behavior in the *o*-phenylenes is offset aromatic interactions directed along the helical axis. In other words, *o*-phenylenes can be considered as analogues of α-helices, with hydrogen bonding replaced by axial arene−arene stacking. This assertion does not necessarily mean that other interactions are insignificant (e.g., edge-to-face interactions in the BAB conformer); rather, we believe that they are not the deciding factor in determining the conformational distribution. *o*-Phenylenes are therefore similar to related foldamers exploiting aromatic stacking, such as Iverson's aedamers.[59] This assertion is supported by several pieces of experimental and computational evidence.

First, the experimental ΔG°_{fold} values for the $\mathbf{oP^6(X)_2}$ series are consistent with a single offset aromatic stacking interaction as the differentiating factor between the AAA and AAB conformers. Accounting for symmetry, the AAA conformer is stabilized 0.3−1.1 kcal/mol relative to AAB, depending on the substituent. These values are in good agreement with the strength of a single aromatic stacking interaction in chloroform, as measured by Hunter using chemical double mutant cycles,[54,55] Gung using molecular torsion balances,[60] and Diederich using the self-assembly of adenine-based receptors.[61] Interestingly, the overall strength of the arene−arene interactions is also directly comparable to the contribution of a phenylalanine−phenylalanine aromatic interaction to the stability of α-helices in peptides.[62]

Second, the variation of of ΔG°_{fold} with σ_m is consistent with a single aromatic stacking interaction at the oligomer ends. The overall trend, increasing interaction (more negative ΔG°_{fold}) with increasing electron-withdrawing power of the substituent, is exactly as expected for aromatic stacking interactions on the basis of the popular Hunter−Sanders[63] and Cozzi−Siegel[53,64,65] models and is broadly consistent with gas-phase computational studies.[45,66−68] This trend has been observed in many model systems designed explicitly to probe these effects.[54,55,60,69] Moreover, the overall substituent effect of roughly 1 kcal/mol for the substituents considered here ($\Delta G^\circ_{fold}(\mathbf{oP^6(CN)_2}) - \Delta G^\circ_{fold}(\mathbf{oP^6(Me)_2})$) is in very good agreement with the magnitude of substituent effects in closely related systems.[54,55,60] Again, as these other systems were explicitly designed to examine individual arene−arene stacking forces, this similarity suggests that the difference between the AAB and AAA conformers is determined by a single such interaction.

Third, further evidence for the deterministic role of arene stacking in these systems comes from the B97-D DFT calculations. Superficially, the simple observation that this method correctly predicts the relative stabilities of the conformers, whereas more common methods such as B3LYP do not, implicates an important role for dispersion interactions in these systems. The influence of the substituents on rotation about the biaryl bonds, another possible effect, does not explain the observed substituent effect, as substituents should have very little effect on the preferred dihedral angles ϕ_2/ϕ_4 (see Supporting Information, Figure S2). More significantly, the ΔE_{fold} values for the AAB ⇄ AAA equilibrium are correlated to a single geometric variable from just the AAA conformer, the centroid−centroid stacking distance (R_{Cn-Cn}) corresponding to the offset stacking interaction at the oligomer terminus, as shown in Figure 7

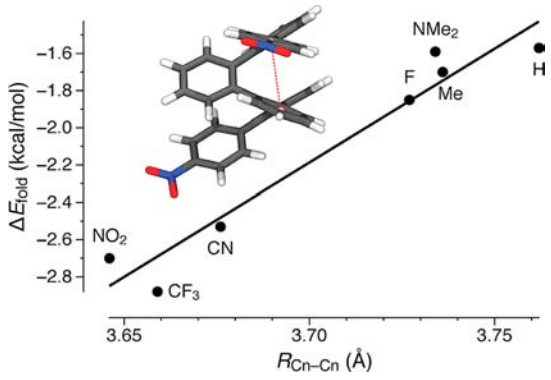

Figure 7. ΔE_{fold} plotted against the centroid−centroid distance R_{Cn-Cn}, depicted as the dashed line in the model of $\mathbf{oP^6(NO_2)_2}$.

($r = 0.97$). Put another way, the overall conformational stability of the perfectly folded AAA conformer is highly correlated to the separation between the rings at the oligomer ends, which should reflect the strength of the arene−arene stacking interaction.

Generalization of these results from the oligomer termini to the *o*-phenylenes as a class may be done by examining the complete conformational space for the oligomers. Thus, the relative energies ΔE_{rel} of all six possible conformers for $\mathbf{oP^6(H)_2}$ (i.e., Figure 3) were compared, taking the most stable AAA state as the reference. Of the six, the ABA conformer is exceptionally unstable (17.5 kcal/mol less stable than AAA): this particular sequence of dihedrals forces the two terminal rings into each other, imparting significant steric strain. The relative energies of the remaining conformers (AAA, AAB, BAB, ABB, BBB) have a simple relationship to the backbone geometry. As shown in Figure 8, ΔE_{rel} shows a good linear dependence on the number of B states in each oligomer ($r = 0.97$), which is easily rationalized as each B state defect would be expected to eliminate exactly one stacking interaction. The slope of the plot, 2.1 ± 0.2 kcal/mol per B state, confirms that each B state breaks one stacking interaction, as it is a good match for the reference value of 2.75 kcal/mol for the breaking of a parallel-displaced benzene dimer at the B97-D/TZV(2d,2p) level.[44] The difference likely

dx.doi.org/10.1021/ja4026006 | J. Am. Chem. Soc. 2013, 135, 6714−6722

results from geometric constraints placed on the interaction by the *o*-phenylene backbone.

This analysis is readily extended to longer *o*-phenylenes. In Figure 8, we also show the relative energies of the conformers of

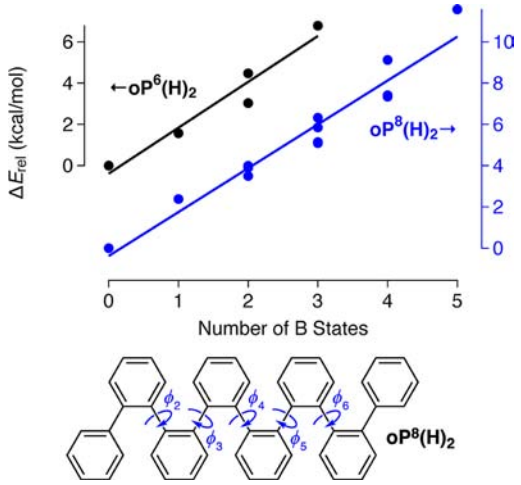

Figure 8. Relative conformer energies ΔE_{rel} for **oP^6(H)$_2$** (black, left) and **oP^8(H)$_2$** (blue, right) plotted against the number of B states. The ΔE_{rel} scales are identical, but the data for **oP^6(H)$_2$** are offset by +4 kcal/mol for clarity.

oP^8(H)$_2$. All possible conformers that do not have ABA sequences are included. A good linear dependence on the number of B states is again observed. The linear fit is parallel to that for the **oP^6(H)$_2$** conformers, at 2.2 ± 0.4 kcal/mol per B state, again suggesting that each B state defect breaks one stacking interaction relative to the AAAAA conformer. Of course, on the basis of the previous comparison of ΔG°_{fold} and ΔE_{fold}, it is clear that these gas-phase enthalpy calculations overestimate the actual preference for the helical conformer, presumably because they omit the effect of solvent.

Taken together, these observations suggest that the conformational behavior of *o*-phenylenes can be understood using a very simple model with two rules. (1) ABA sequences are prohibited as they require the backbone to contort into a structure with high steric strain. (2) The relative energies of the remaining conformers are determined by offset arene−arene stacking interactions that are a simple additive function of the number of A states along the backbone.

Our experimental ΔG°_{fold} values suggest that these interactions are stabilizing by roughly 0.5 kcal/mol for the parent (unsubstituted) *o*-phenylenes but are sensitive to substituent effects. This model reproduces the observed complete conformational distribution of **oP^6(H)$_2$** very well: a stacking interaction of −0.47 kcal/mol predicts a conformer distribution at 277 K of 49:42:9 for AAA:AAB:BAB, a perfect match for the experimentally observed population.[70]

While this simple model accounts for the preference for helical conformations in the *o*-phenylenes in a general sense, it can be used to treat specific aspects of their folding behavior. For example, we have previously shown that the conformational population of long *o*-phenylenes favors the compact helix and a minor "frayed ends" state in which one of the termini is flipped from the helical path. Put another way, for an *o*-phenylene [*n*]-mer, the A_{n-1} conformer (AA...AA) is the major conformer and the $A_{n-2}B$ conformer (AA...AB) is always the next most populated. For one series of oligomers, this behavior has been confirmed in oligomers up to the dodecamer;[24] similar behavior has been reported by Fukushima and Aida.[26] The reason for this "frayed ends" behavior of the *o*-phenylenes is easily rationalized. The two rules described above require that the second-most stable conformation of an *o*-phenylene have a single B state (maximizing stacking interactions via rule 2) and that this B configuration be located at the end, since internal isolated B defects require ABA sequences which are forbidden (rule 1).

The overall conformer population will favor well-defined helical folding so long as the number of backbone conformers with two or more B states does not entropically swamp the enthalpic preference for helical folding. To examine the overall folding behavior of the *o*-phenylenes in more detail, we estimated the equilibrium fraction of "well-folded" oligomers as a function of oligomer length (*n*) and arene−arene interaction energy assuming the simple model above. We define "well-folded" to include the perfectly folded conformer (e.g., AAAAA) as well as those with defects only at the very ends (e.g., AAAAB and BAAAB). Thus, there are three "well-folded" conformers for each oligomer regardless of *n* ($n \geq 6$). Every possible backbone configuration for oligomers up to the [30]-mer was considered explicitly using a simple computer algorithm (see Supporting Information). The results are shown in Figure 9.

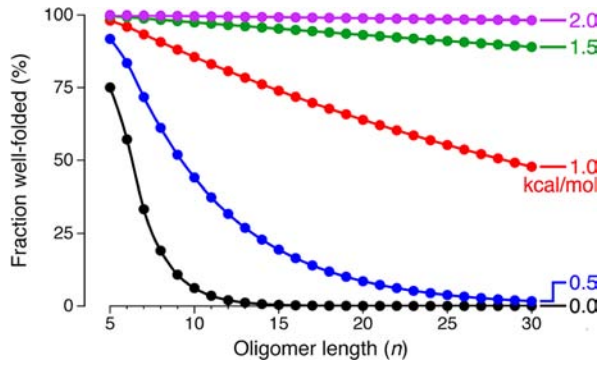

Figure 9. Equilibrium fraction of total population in well-folded conformations as a function of oligomer length up to the [30]-mer, shown for different values of arene−arene stacking stabilization (0.0, 0.5, 1.0, 1.5, and 2.0 kcal/mol).

This model is, of course, idealized, but makes some useful predictions with respect to *o*-phenylene folding. In the absence of any stabilization by arene−arene interactions (black curve in Figure 9), the occurrence of well-folded conformers is a function of simple statistics, and since the number of backbone configurations increases exponentially with *n*, their fraction of the total population decreases rapidly with increasing length. However, interactions with strengths typical of arene−arene stacking are expected to have a significant impact on the overall distribution. Arene−arene stabilization of 0.5 kcal/mol per interaction (blue curve), as expected for the parent series of oligomers, shifts the population toward the well-folded states, although the folded population does still decrease significantly with length. Therefore, the parent poly(*o*-phenylene) should exist as short helical segments interrupted by many defect states. An increase in the stabilization energy to 1.0 kcal/mol per interaction (red curve), accessible by strengthening the aromatic interactions through simple substitution with electron-withdrawing groups (Figure 5), should have a substantial effect on the conformational population and give oligomers with much better folding properties. A further increase in stabilization to

dx.doi.org/10.1021/ja4026006 | *J. Am. Chem. Soc.* 2013, 135, 6714−6722

1.5−2.0 kcal/mol per interaction, attainable through noncovalent interactions such as hydrogen bonding, would yield oligomers and polymers with a very high fraction of perfect folding. This sensitivity of the conformational behavior may also, in part, explain the observation by Fukushima and Aida of solvent-dependent "perfect" folding for their oligomers,[26] since significant changes in solvation energy could have a dramatic effect on the folding propensity.

This model has implications for the mechanism of *o*-phenylene racemization, a topic of interest given the remarkable behavior of the resolved *o*-phenylenes reported by Fukushima and Aida.[25,26] We assume here that racemization occurs via the B states (for which a single, facile torsional motion converts to the inverted B′ state). Since isolated B states in the center of the chain are forbidden, defects may originate at the ends of the chain and effectively nucleate the formation of additional defect states along the backbone. Interestingly, Fukushima and Aida have measured free energies of activation for racemization $\Delta G^{\ddagger}_{rac}$ for one of their series of *o*-phenylenes. The $\Delta G^{\ddagger}_{rac}$ values increase linearly with increasing oligomer length up to the octamer, with an increment of 0.45 kcal/mol per arylene unit. This value is in good agreement with the model, assuming that the transition state for racemization of *o*-phenylene oligomers essentially involves simultaneous breaking of all the stabilizing arene−arene interactions.

Given the success of the B97-D calculations of reproducing the conformational behavior of the $\mathbf{oP^6(X)_2}$ series, we were interested in comparing the parent *o*-phenylenes to those examined by Fukushima and Aida,[25,26] which typically have been based on veratrole repeat units. Thus, we carried out geometry optimizations of a representative hexamer $\mathbf{oP^6(FA)}$.[71] Because rotation about the terminal biaryl bonds in this series is not degenerate, all possible orientations of the end groups for the AAA, AAB, BAB, ABB, and BBB conformers were optimized explicitly (see the Supporting Information).[72] Energies of the individual backbone configurations were obtained by taking the Boltzmann averages. The conformer stabilities were then compared to those for the parent hexamer $\mathbf{oP^6(H)_2}$, as shown in Figure 10. For the purposes of this comparison, the BBB

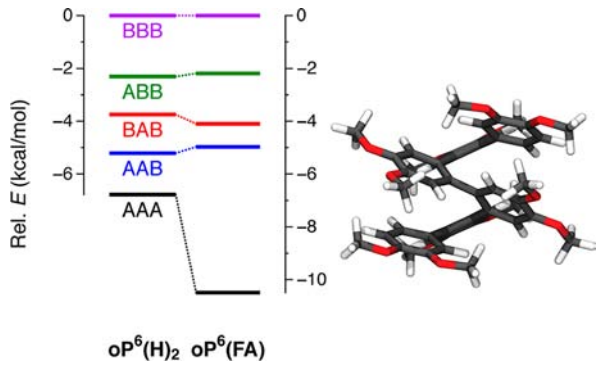

Figure 10. Left: conformer energies of $\mathbf{oP^6(FA)}$ compared to $\mathbf{oP^6(H)_2}$, relative to the BBB state. Right: geometry of the lowest-energy AAA conformer of $\mathbf{oP^6(FA)}$.

conformer (i.e., the least stable), was chosen as a convenient reference state as it should be essentially free of stacking interactions in either case.

The calculated energies reveal a substantial difference in behavior between the two prototypical *o*-phenylenes. Most of the conformations (ABB, BAB, AAB) have very similar stabilities

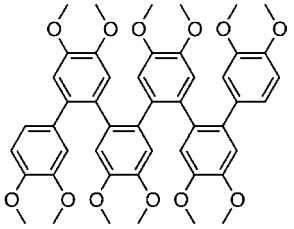

relative to the BBB state. However, the perfectly folded AAA conformer is substantially more stable for $\mathbf{oP^6(FA)}$, suggesting that this series is much more prone to well-defined folding at the termini compared to other *o*-phenylenes. At first glance, this stabilization of the AAA conformer would appear to contradict our model of additive arene−arene stacking interactions. However, the reason for the enhanced stability of the $\mathbf{oP^6(FA)}$ AAA state is the asymmetry of the terminal arenes: the most stable conformer, shown in Figure 10, is that for which these groups are rotated such that the methoxy groups are out of alignment with those in the center of the oligomer. Inspection of the electrostatic potential map for veratrole (Figure S3) does not provide an obvious explanation for this preference in terms of the electronic distribution of the π-system in the repeat units; it is most easily rationalized in the context of direct repulsive interactions between the methoxy groups,[45] which are much farther apart in the most stable conformer. While this result for $\mathbf{oP^6(FA)}$ is purely computational, it may explain, in a general sense, the many exceptional properties Fukushima, Aida, and coworkers have observed for various veratrole-derived *o*-phenylenes: these heavily substituted oligomers may represent a privileged class of *o*-phenylenes with exceptional folding properties at their ends, which may be key sites for controlling racemization mechanisms (see above). This result also underscores the potential role of substituent effects in modulating the aromatic stacking interactions in polyphenylenes as a class and *o*-phenylenes in particular.

CONCLUSIONS

In summary, a series of *o*-phenylene hexamers with varying substitution at their ends has been synthesized. The substituent effect on the conformational distributions of these oligomers demonstrates that the key determinant of the folding properties of *o*-phenylenes is offset arene−arene stacking interactions between every third repeat unit. The B97-D/TZV(2d,2p) DFT method accurately predicts these substituent effects. Analysis of different model systems suggests that the relative stabilities of different *o*-phenylene conformers are predicted by two simple rules: (1) ABA sequences are disallowed because they contort the backbone into a highly sterically strained conformation, and (2) arene−arene stacking interactions are essentially an additive function of the number of A states. For the parent oligomer, the net stabilization of each stacking interaction is approximately 0.5 kcal/mol, a value derived from the observed conformational population of the hexamer and in excellent agreement with expectations for aromatic stacking interactions in chloroform. This model rationalizes the observed behavior of current *o*-phenylene oligomers, and predicts that *o*-phenylene folding should be very sensitive to relatively small perturbations of the strengths of the arene−arene interactions. If the *o*-phenylenes are taken as representatives of polyphenylenes in general, this study demonstrates that the folding behavior of polyphenylenes, despite apparent complexity, may be amenable to very simple

dx.doi.org/10.1021/ja4026006 | J. Am. Chem. Soc. 2013, 135, 6714−6722

models. Further, modern, diffusion-corrected DFT methods, such as B97-D/TZV(2d,2p), do an excellent job of predicting the relative stability of polyphenylene conformers. Both of these results may be of use in designing polyphenylenes with functional tertiary structures.

■ ASSOCIATED CONTENT

Supporting Information

Supplemental figures referred to in the text; crystal data for $oP^6(Me)_2$, $oP^6(NMe_2)_2$, $oP^6(NO_2)_2$, and $oP^6(CF_3)_2$; NMR spectra at 277 K for $oP^6(X)_2$ with chemical shift assignments; experimental procedures; computational energies and optimized geometries. This material is available free of charge via the Internet at http://pubs.acs.org.

■ AUTHOR INFORMATION

Corresponding Author

scott.hartley@miamioh.edu

Notes

The authors declare no competing financial interest.

■ ACKNOWLEDGMENTS

C.S.H. and S.M.M. acknowledge support by the National Science Foundation (CHE-0910477). Gaussian 09 was purchased with the assistance of the Air Force Office of Scientific Research (FA9550-10-1-0377). We thank Prof. Steven Wheeler for help obtaining the TZV(2d,2p) basis set. C.J.Z. acknowledges the National Science Foundation (CHE-0840446) for funds used to purchase the Bruker ApexII Duo CCD X-ray diffractometer.

■ REFERENCES

(1) Berresheim, A. J.; Müller, M.; Müllen, K. *Chem. Rev.* **1999**, *99*, 1747−1786.
(2) Schmaltz, B.; Weil, T.; Müllen, K. *Adv. Mater.* **2009**, *21*, 1067−1078.
(3) Omachi, H.; Segawa, Y.; Itami, K. *Acc. Chem. Res.* **2012**, *45*, 1378−1389.
(4) Kandre, R.; Feldman, K.; Meijer, H. E. H.; Smith, P.; Schlüter, A. D. *Angew. Chem., Int. Ed.* **2007**, *46*, 4956−4959.
(5) Banerjee, M.; Shukla, R.; Rathore, R. *J. Am. Chem. Soc.* **2009**, *131*, 1780−1786.
(6) Ivory, D. M.; Miller, G. G.; Sowa, J. M.; Shacklette, L. W.; Chance, R. R.; Baughman, R. H. *J. Chem. Phys.* **1979**, *71*, 1506−1507.
(7) Grimsdale, A. C.; Leok Chan, K.; Martin, R. E.; Jokisz, P. G.; Holmes, A. B. *Chem. Rev.* **2009**, *109*, 897−1091.
(8) Weiss, E. A.; Ahrens, M. J.; Sinks, L. E.; Gusev, A. V.; Ratner, M. A.; Wasielewski, M. R. *J. Am. Chem. Soc.* **2004**, *126*, 5577−5584.
(9) Bhosale, S.; Sisson, A. L.; Talukdar, P.; Fürstenberg, A.; Banerji, N.; Vauthey, E.; Bollot, G.; Mareda, J.; Röger, C.; Würthner, F.; Sakai, N.; Matile, S. *Science* **2006**, *313*, 84−86.
(10) Reddinger, J. L.; Reynolds, J. R. *Macromolecules* **1997**, *30*, 479−481.
(11) Ben, T.; Goto, H.; Miwa, K.; Goto, H.; Morino, K.; Furusho, Y.; Yashima, E. *Macromolecules* **2008**, *41*, 4506−4509.
(12) Goto, H.; Katagiri, H.; Furusho, Y.; Yashima, E. *J. Am. Chem. Soc.* **2006**, *128*, 7176−7178.
(13) Goto, H.; Furusho, Y.; Yashima, E. *J. Am. Chem. Soc.* **2007**, *129*, 9168−9174.
(14) Miwa, K.; Furusho, Y.; Yashima, E. *Nat. Chem.* **2010**, *2*, 444−449.
(15) Bauer, R. E.; Grimsdale, A. C.; Müllen, K. *Top. Curr. Chem.* **2005**, *245*, 253−286.
(16) Weil, T.; Reuther, E.; Müllen, K. *Angew. Chem., Int. Ed.* **2002**, *41*, 1900−1904.
(17) Nguyen, T.-T.-T.; Türp, D.; Wang, D.; Nölscher, B.; Laquai, F.; Müllen, K. *J. Am. Chem. Soc.* **2011**, *133*, 11194−11204.
(18) Wittig, G.; Lehmann, G. *Chem. Ber.* **1957**, *90*, 875−892.
(19) Ozasa, S.; Fujioka, Y.; Fujiwara, M.; Ibuki, E. *Chem. Pharm. Bull.* **1980**, *28*, 3210−3222.
(20) Kovacic, P.; Uchic, J. T.; Hsu, L.-C. *J. Polym. Sci., Part A: Polym. Chem.* **1967**, *5*, 945−964.
(21) He, J.; Crase, J. L.; Wadumethrige, S. H.; Thakur, K.; Dai, L.; Zou, S.; Rathore, R.; Hartley, C. S. *J. Am. Chem. Soc.* **2010**, *132*, 13848−13857.
(22) Mathew, S. M.; Hartley, C. S. *Macromolecules* **2011**, *44*, 8425−8432.
(23) He, J.; Mathew, S. M.; Cornett, S. D.; Grundy, S. C.; Hartley, C. S. *Org. Biomol. Chem.* **2012**, *10*, 3398−3405.
(24) Hartley, C. S.; He, J. *J. Org. Chem.* **2010**, *75*, 8627−8636.
(25) Ohta, E.; Sato, H.; Ando, S.; Kosaka, A.; Fukushima, T.; Hashizume, D.; Yamasaki, M.; Hasegawa, K.; Muraoka, A.; Ushiyama, H.; Yamashita, K.; Aida, T. *Nat. Chem.* **2011**, *3*, 68−73.
(26) Ando, S.; Ohta, E.; Kosaka, A.; Hashizume, D.; Koshino, H.; Fukushima, T.; Aida, T. *J. Am. Chem. Soc.* **2012**, *134*, 11084−11087.
(27) Nakano, T.; Okamoto, Y. *Chem. Rev.* **2001**, *101*, 4013−4038.
(28) Yashima, E.; Maeda, K.; Iida, H.; Furusho, Y.; Nagai, K. *Chem. Rev.* **2009**, *109*, 6102−6211.
(29) Gellman, S. H. *Acc. Chem. Res.* **1998**, *31*, 173−180.
(30) Hill, D. J.; Mio, M. J.; Prince, R. B.; Hughes, T. S.; Moore, J. S. *Chem. Rev.* **2001**, *101*, 3893−4012.
(31) Guichard, G.; Huc, I. *Chem. Commun.* **2011**, *47*, 5933−5941.
(32) Arslan, H.; Saathoff, J. D.; Bunck, D. N.; Clancy, P.; Dichtel, W. R. *Angew. Chem., Int. Ed.* **2012**, *51*, 12051−12054.
(33) Manabe, K.; Kimura, T. *Org. Lett.* **2013**, *15*, 374−377.
(34) Chen, L.; Hernandez, Y.; Feng, X.; Müllen, K. *Angew. Chem., Int. Ed.* **2012**, *51*, 7640−7654.
(35) Yan, X.; Li, L.-S. *J. Mater. Chem.* **2011**, *21*, 3295−3300.
(36) Pradhan, A.; Dechambenoit, P.; Bock, H.; Durola, F. *J. Org. Chem.* **2013**, *78*, 2266−2274.
(37) Zhou, Q. J.; Worm, K.; Dolle, R. E. *J. Org. Chem.* **2004**, *69*, 5147−5149.
(38) Shintani, R.; Maciver, E. E.; Tamakuni, F.; Hayashi, T. *J. Am. Chem. Soc.* **2012**, *134*, 16955−16958.
(39) Blake, A.; Cooke, P.; Doyle, K.; Gair, S.; Simpkins, N. *Tetrahedron Lett.* **1998**, *39*, 9093−9096.
(40) In previous publications, we assigned a value of ±70° to the A state. Here, we revise this value to ±55° in light of the new computational optimized geometries and crystal structures.
(41) Kristyán, S.; Pulay, P. *Chem. Phys. Lett.* **1994**, *229*, 175−180.
(42) Johnson, E. R.; Wolkow, R. A.; DiLabio, G. A. *Chem. Phys. Lett.* **2004**, *394*, 334−338.
(43) Hobza, P.; Šponer, J.; Reschel, T. *J. Comput. Chem.* **1995**, *16*, 1315−1325.
(44) Grimme, S. *J. Comput. Chem.* **2006**, *27*, 1787−1799.
(45) Wheeler, S. E. *J. Am. Chem. Soc.* **2011**, *133*, 10262−10274.
(46) Vázquez-Mayagoitia, A.; Sherrill, C. D.; Aprà, E.; Sumpter, B. G. *J. Chem. Theory Comput.* **2010**, *6*, 727−734.
(47) Grimme, S.; Antony, J.; Schwabe, T.; Mück-Lichtenfeld, C. *Org. Biomol. Chem.* **2007**, *5*, 741−758.
(48) Wiitala, K. W.; Hoye, T. R.; Cramer, C. J. *J. Chem. Theory Comput.* **2006**, *2*, 1085−1092.
(49) Jain, R.; Bally, T.; Rablen, P. R. *J. Org. Chem.* **2009**, *74*, 4017−4023.
(50) Exner, O. In *Correlation Analysis in Chemistry: Recent Advances*; Chapman, N. B., Shorter, J., Eds.; Plenum Press: New York, 1978; pp 439−540.
(51) Salonen, L. M.; Ellermann, M.; Diederich, F. *Angew. Chem., Int. Ed.* **2011**, *50*, 4808−4842.
(52) Mati, I. K.; Cockroft, S. L. *Chem. Soc. Rev.* **2010**, *39*, 4195.
(53) Cozzi, F.; Cinquini, M.; Annuziata, R.; Siegel, J. S. *J. Am. Chem. Soc.* **1993**, *115*, 5330−5331.
(54) Cockroft, S. L.; Hunter, C. A.; Lawson, K. R.; Perkins, J.; Urch, C. J. *J. Am. Chem. Soc.* **2005**, *127*, 8594−8595.

(55) Cockroft, S. L.; Perkins, J.; Zonta, C.; Adams, H.; Spey, S. E.; Low, C. M. R.; Vinter, J. G.; Lawson, K. R.; Urch, C. J.; Hunter, C. A. *Org. Biomol. Chem.* **2007**, *5*, 1062−1080.
(56) Fischer, F. R.; Schweizer, W. B.; Diederich, F. *Chem. Commun.* **2008**, 4031−4033.
(57) Graton, J.; Le Questel, J.-Y.; Legouin, B.; Uriac, P.; van de Weghe, P.; Jacquemin, D. *Chem. Phys. Lett.* **2012**, *522*, 11−16.
(58) Hawkins, G. D.; Cramer, C. J.; Truhlar, D. G. *J. Phys. Chem. B* **1998**, *102*, 3257−3271.
(59) Lokey, R. S.; Iverson, B. L. *Nature* **1995**, *375*, 303−305.
(60) Gung, B. W.; Xue, X.; Reich, H. J. *J. Org. Chem.* **2005**, *70*, 3641−3644.
(61) Faraoni, R.; Blanzat, M.; Kubicek, S.; Braun, C.; Schweizer, W. B.; Gramlich, V.; Diederich, F. *Org. Biomol. Chem.* **2004**, *2*, 1962−1964.
(62) Butterfield, S. M.; Patel, P. R.; Waters, M. L. *J. Am. Chem. Soc.* **2002**, *124*, 9751−9755.
(63) Hunter, C. A.; Sanders, J. K. M. *J. Am. Chem. Soc.* **1990**, *112*, 5525−5534.
(64) Cozzi, F.; Cinquini, M.; Annunziata, R.; Dwyer, T.; Siegel, J. S. *J. Am. Chem. Soc.* **1992**, *114*, 5729−5733.
(65) Cozzi, F.; Ponzini, F.; Annunziata, R.; Cinquini, M.; Siegel, J. S. *Angew. Chem., Int. Ed. Engl.* **1995**, *34*, 1019−1020.
(66) Wheeler, S. E.; Houk, K. N. *J. Am. Chem. Soc.* **2008**, *130*, 10854−10855.
(67) Watt, M.; Hardebeck, L. K. E.; Kirkpatrick, C. C.; Lewis, M. *J. Am. Chem. Soc.* **2011**, *133*, 3854−3862.
(68) Sinnokrot, M. O.; Sherrill, C. D. *J. Am. Chem. Soc.* **2004**, *126*, 7690−7697.
(69) Cozzi, F.; Annunziata, R.; Benaglia, M.; Cinquini, M.; Raimondi, L.; Baldridge, K. K.; Siegel, J. S. *Org. Biomol. Chem.* **2003**, *1*, 157−162.
(70) This population is derived from the following: $\Delta G^{\circ}_{1} = -0.47 + 0.38 = -0.09$ kcal/mol for the equilibrium AAB ⇄ AAA and $\Delta G^{\circ}_{2} = -0.47 - 0.38 = -0.95$ kcal/mol for the equilibrium BAB ⇄ AAB at 277 K. The contributions of 0.38 kcal/mol arise from symmetry considerations ($-RT \ln(1/2)$). Of course, this is an idealized model: we would expect to observe more of the ABB conformer, but evidently its small deviation from the −0.47 kcal/mol assumed for the stacking interaction reduces its population below the detection limit of the experiment. This deviation is predicted by the B97-D calculations.
(71) Ormsby, J. L.; Black, T. D.; Hilton, C. L.; Bharat; King, B. T. *Tetrahedron* **2008**, *64*, 11370−11378.
(72) The ABA conformers were ignored, for the reasons described above.